J Mater Sci (2007) 42:8193–8202
DOI 10.1007/s10853-007-1694-7

Preparation of anatase F doped TiO_2 sol and its performance for photodegradation of formaldehyde

Donggen Huang · Shijun Liao · Shuiqing Quan · Lei Liu · Zongjian He · Jinbao Wan · Wenbin Zhou

Received: 12 August 2006 / Accepted: 15 March 2007 / Published online: 9 June 2007

Abstract Anatase fluoride doped TiO_2 sol (F-TiO_2) catalyst was prepared by a modified sol-gel hydrothermal method, using tetra butyl titanate as a precursor. The influences of F doping, temperature of hydrothermal, values of medium pH on the morphology and crystallization were studied. The microstructure and morphology of sol sample were characterized by XRD, TEM, FTIR, UV–Vis–DRS, particle size distribution (PSD) and XPS. The results showed that F-TiO_2 particles in sol were spherical and partly crystallized to anatase structure, and dispersed in the aqueous medium homogeneously and that the average particle size was ca. 10.5 nm calculated from XRD and TEM results. It was also found that the addition of fluorine could improve the crystallization and adsorption of particles significantly, the photocatalytic activity for decomposition of formaldehyde were enhanced remarkably with the doping of fluorine. Possible mechanism of anatase F-TiO_2 formed under hydrothermal conditions was discussed.

D. Huang (✉) · S. Quan · L. Liu · Z. He · J. Wan · W. Zhou
School of Environmental Science and Engineering, The Key Lab of Poyang Lake ecology and Bio-resource Utilization Ministry of Education, Nanchang University, Nanchang 330031, China
e-mail: dghuang1017@163.com

S. Liao
College of Chemistry, South China University of Technology, Guangzhou 510640, China

Introduction

Compared with powder state TiO_2 photocatalyst, TiO_2 sol catalyst has several advantages: (1) Better dispersion in water, final particle size with more uniform distribution and small particle itself; (2) High photocatalytic activity; (3) Easy coating on different supporting materials including those substrates with a poor thermal resistance such as some polymers, optical fibers, plastics, woods, porcelains, tiles, and papers. Hereby, much attention has been focused on the anatase TiO_2 sol photocatalyst [1–3]. However, it is generally believed that most sol without high temperature treatment has an amorphous structure, and the amorphous TiO_2 has poor photoactivity; in addition, the crystal phase of TiO_2 is also a critical factor and the anatase phase usually shows a better photoactivity than the rutile phase [4]. On the other hand, surface acidity and adsorption capacity are important factors that may influence the photocatalytic activity of TiO_2 for the photodegradation of environmental pollutant [5]. Therefore, it is very important to study how to prepare anatase TiO_2 sol catalyst on facile conditions.

There were many investigative reports on TiO_2 sol photocatalysts that were related to the preparation [1], characterization [2], modification, and application [3]. Based on the report of literatures, the preparation of TiO_2 sol photocatalyst had several methods, such as: dispersion of TiO_2 powder method [6], sol-gel-thermal method [7], sol-gel-peptization method [8], gel-peptization method [9]. Like TiO_2 powder photocatalyst, the doping of TiO_2 sol particles was an effective means to improve its photocatalytic activity, and the transition metals [10], rare earth metal ions [11], noble metals were the main doping elements [12]. As we know, although anions doping TiO_2 powder catalysts had been reported by many investigators

[13, 14], the preparation of anatase F doped TiO_2 sol by sol-gel -hydrothermal method has not been reported.

In this work, fluoride ion doping TiO_2 sol (F-TiO_2) catalysts was fabricated by a modified sol-gel hydrothermal method, using tetra butyl titanate as a precursor. The catalysts were characterized with XRD, TEM, FTIR, UV-Vis-DRS, particle size distribution (SPD), and XPS. The influences of F doping on the crystallinity, absorption capacity of F-TiO_2 sol particles and its degradation performance for formaldehyde were investigated in detail. Possible mechanism of anatase F-TiO_2 formed under hydrothermal conditions was discussed.

Experimental

Preparation of F-TiO_2 sol

Tetrabutyl titanate was used as a starting material and ammonium fluoride as a fluorine source. All chemicals used in the experiments were analytical reagent grade. First, precursor tetrabutyl titanate (20 mL), 10 mL of ethanol and 5.0 mL acetic acid were accurately measured and put into a 200 mL flask with stirring for 30 min to form solution A; ammonium fluoride, the atomic ratios of F to Ti were in the range of 0.01–0.08, 6 mL ultra pure water obtained with a Millipore system (Milli Q-50 18 MΩ). About 2.0 mL nitric acid and 80.0 mL ethanol were mixed with stirring for 10 min to form solution B. Second, solution B was added dropwise into solution A under vigorous stirring. After finishing addition, slow stirring had been continued until the solution formed a transparent immobile gel. The obtained gel was dispersed in water to form a sol mixture. Finally, the sol mixture was placed into a Teflon tube that was then placed in a 300 cm^3 stainless steel autoclave. The autoclave was heated in an oven and kept at 140–190 °C for 6–10 h. After ultrasonic treatment, the obtained product formed uniform, stable, and semitransparent sol. The acquired F-TiO_2 sol could maintain homogenous dispersion for quite a long time without sedimentation and delamination phenomena. In order to compare, a pure F-TiO_2 sol sample was prepared using hydrofluoric acid as fluorine source. In addition, a pure TiO_2 sol sample was also prepared in the same procedure.

Characterization

The phase of composition, crystal structure and particle size of the prepared TiO_2 sol particles dried in a rotatory evaporator at 60 °C and then dried in vacuum at 60 °C for 36 h were analyzed by using a X-ray powder diffractometer (XD-3A, Shimadazu Corporation, Japan) with graphite monochromatic copper radiation (Cu K_α λ = 0.15418 nm), 30 kV as accelerating voltage, 30 mA as emission current over the 2θ range 20–50°.

Scherer's equation was used to calculate the particle size of titanium dioxide crystal:

$$D = k\lambda/\beta\cos\theta$$

Where D is crystallite particle size, k is a constant of 0.89, $\lambda$is X-ray wavelength (0.15418 nm), β is half maximum line breadth, and θ is Bragg angle.

Morphology and size of the TiO_2 sol particles were also examined by transmission electron microscopy (TEM), the TiO_2 sol was deposited on a copper mesh by means of dip-coating and placed several days in room temperature.

The particle size distribution was determined by light scattering size analyzer (Zetasizer 3000HSA, Malvern Instruments Ltd., Worcs, United Kingdom).

UV–Vis absorption spectra of F-TiO_2 sol sample powders dried in a rotatory evaporator at 60 °C and then dried in vacuum at 60 °C for 36 h were obtained for the dry-pressed disk samples using a UV–Visible spectrophotometer with an integrating sphere (UV-3010, HITACHI). Absorption spectra were referred to $BaSO_4$.

Infrared absorption spectra were recorded for KBr disks containing sol sample powder dried in a rotatory evaporator at 60 °C and then dried in vacuum at 60 °C for 36 h with an FTIR spectrometer (Tensor 27, Bruker).

X-ray photoelectron spectroscopy (XPS) measurements were performed with the PHI1600 Quantum ESCA Microprobe System, using the Mg_K. Line of a 300W Mg X-ray tube as a radiation source at 15 kV. All the binding energies were referred to the C 1s peak at 284.8 eV of the surface adventitious carbon. The F-TiO_2 sol sample dried in a rotatory evaporator at 60 °C, and then dried in vacuum at 60 °C for 36 h, finally, pretreated under an O_2 flow at 320 °C for 6 h, in order to completely decompose and remove any possible precursor residues and organic contaminants.

F-TiO_2 particle crystallinity was determined. Part of the F-TiO_2 sol sample powder dried in a rotatory evaporator at 60 °C and then dried in vacuum at 60 °C for 36 h was calcined at 450 °C in a box furnace for 6 h. Therefore, the F-TiO_2 particle's crystallinity was defined as 100%, and was used as the standard reference sample for the determination of sample crystallinity. The relative crystallinity of the various samples was calculated as follows:

$$R\% = I_{(101peak)}/I_{0(101peak)} \times 100$$

Where I is the anatase TiO_2 peak (101) intensity of the sample and I_0 is standard substance, respectively.

The adsorptive formaldehyde gas was performed volumetrically at 25 °C in a 10 L close glass vessel. TiO_2 powder dried at 120 °C for 6 h was introduced into it, and then formaldehyde was carried out in the closed glass vessel circulation system interfaced to a gas chromatograph (Agilent, 6890N) with a TCD detector. The adsorbed amount of formaldehyde was calculated from the change of formaldehyde concentration in gas phase, i.e., subtracting the residual formaldehyde in gas phase after the adsorption equilibrated from the introduced formaldehyde.

The absorption of colorless materials P-chlorophenol and colored substance Rhodamine B on TiO_2 sol particles was conducted as follows: 0.1000 g of the powder catalyst was soaked in 100 mL 130 mg L^{-1} P-chlorophenol solution, and 0.2000 g of the catalyst was soaked in 25 mL 5 mg L^{-1} Rhodamine B solution respectively, with stirring, at room temperature and neutral pH in dark for 60 min.

The numbers of acid sites on the TiO_2 sol particle surfaces were measured by titrating the TiO_2 suspension in benzene with *n*-buthylamine, using adsorbed Hammett indicator of Methyl Red (pKa = 4.8) to determine the endpoint [15].

Photocatalytic activity measurements

Experimental set-up

A schematic diagram of the experimental system for formaldehyde degradation is shown in Fig. 1a. By the control of the saturator temperature, concentration of formaldehyde solution and the ratio gas flow rates, the obtained formaldehyde gas stream entered the photo reactor was 61 mL min^{-1}, inlet formaldehyde concentration was 1.8 mg m^{-3} and the relative humidity (RH) was in the range of 50–55%.

The cylindrical photoreactor shown in Fig. 1b was made of glass with the diameter of 12 cm and the length of 35 cm, with effective volume 3.5 L. The outside of the photoreactor was a cooling water sleeve to maintain stable reaction temperature. Illumination was provided by 11 w common fluorescent visible light.

The acquired TiO_2 colloidal solution was coated in a thin layer on a set of 30 × 5 cm (i.e., 150 cm^2) tile and placed into the reactor. A uniform thin (average surface density of 0.4 mg $TiO_2 \cdot cm^{-2}$) of catalysts was achieved by spraying the tile with TiO_2 sol and drying at 160 °C for 30 min repeating 3–5 times.

Analyses and procedures

The concentration of formaldehyde was analyzed by the ethylene–acetone spectrometer-photometric method. The gas samples were collected periodically using the mixture of ammonium acetate and ethylene–acetone. All the experimental data were collected under a steady state.

When the concentrations of formaldehyde were constant and the FVL lamp was turned off, the concentration value was the inlet concentration; and the FVL lamp was turned on, the concentration value was the after photodegradation concentration.

The photodegradation of formaldehyde was calculated as follows:

$$D(\%) = 100(C_0 - C)/C_0$$

Where C_0 is the inlet concentration and C is concentration after photodegradation at steady state.

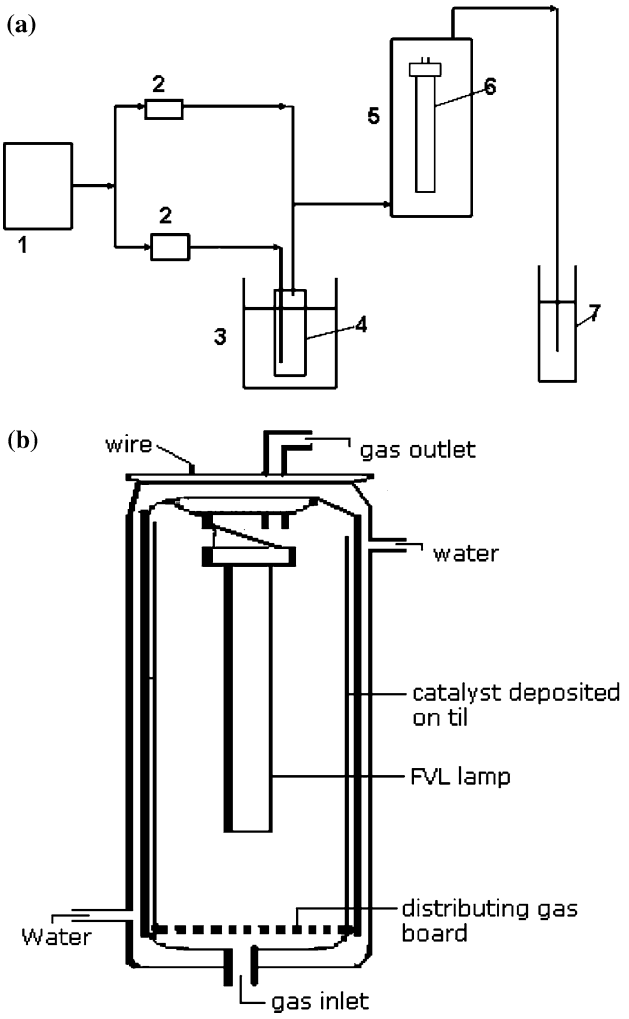

Fig. 1 (**a**) The experimental setup: 1-air supply; 2-air flow controllers; 3-thermostator; 4-formaldehyde; 5-photocatalytic reactor; 6-light source; 7-absorbing liquid (**b**) Schematic diagram of photoreactor designed for formaldehyde degradation

Where C_0 is the inlet concentration, C is the outlet concentration at steady state.

Results and discussion

The particulate morphology, size, and crystallinity

Figure 2 shows the XRD patterns of pure TiO_2 and F-TiO_2 particles. It was found that both pure TiO_2 and F-TiO_2 sol particles had typical XRD patterns and the presence of peaks (2θ = 25.10°, 37.70°, 47.86°), which was regarded as an attributive indicator of anatase titania, and Sol particles only had anatase crystal phase. On the same hydrothermal crystallization treatment conditions (pH value of media: 2.0, 140 °C for 10 h), the F-TiO_2 particles exhibited a stronger diffraction peak at 2θ = 25.10° than pure TiO_2. Using the curve D (shown in Fig. 2d) as a standard, the relative crystallinity of F-TiO_2 sol particles was 62.5%, which was 16.5% higher than that of pure TiO_2. The TiO_2 gel (shown in Fig. 2a), had not any significant peaks representing the characteristic of crystalline, which meant it had a predominant amorphous structure. According to Scherer's equation, the particle size of F-TiO_2 sol was 10.5 nm. These results show that the adding of F can improve the transformation of amorphous to anatase type TiO_2.

TEM photograph showed that F-TiO_2 sol particles with spheroidal shape homogeneously distributed and the average size was about 11.0 nm (shown in Fig. 3). The result corresponded to the XRD testing value, and also meant that little aggregation was among particles in F-TiO_2 sol.

Figure 4 shows the particle size distribution (PSD) of TiO_2 sol. The F-TiO_2 particles in the whole dispersion medium seldom had the same size. It could be found that their sizes might distribute over quite a wide range. Figure 4 shows that the F-TiO_2 sol particles had single-modal distribution characteristic and particle size distributed from 5 to 45 nm with the maximum peak at 12 nm.

Influence of temperature on the crystallization of F-TiO_2 sol particles

Figure 5 presents the XRD patterns of F-TiO_2 sol particles prepared by sol-gel-solvothermal methods under different temperatures, at a pH of 1.5 and at 160 °C for 16 h. The XRD analysis showed that the sol particles obtained from 25 °C hydrothermal reaction temperature were amorphous, and there was no crystal transformation. At 120 °C, the anatase TiO_2 sol particles emerged obviously, the higher the hydrothermal temperature, the higher the crystallinity of TiO_2 sol particles.

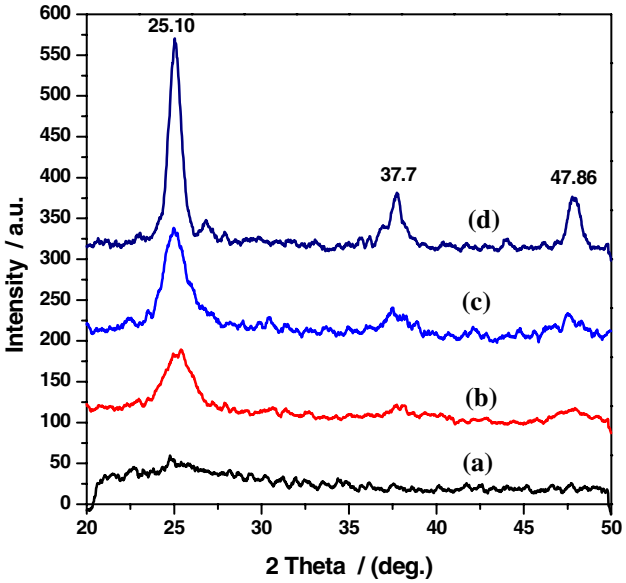

Fig. 2 Effect of F atoms doped on the crystallization of TiO_2 sol particles dried at 60 °C. a: TiO_2 gel; b: TiO_2 sol; c: F-TiO_2 sol; d: F-TiO_2 sintered at 450 °C

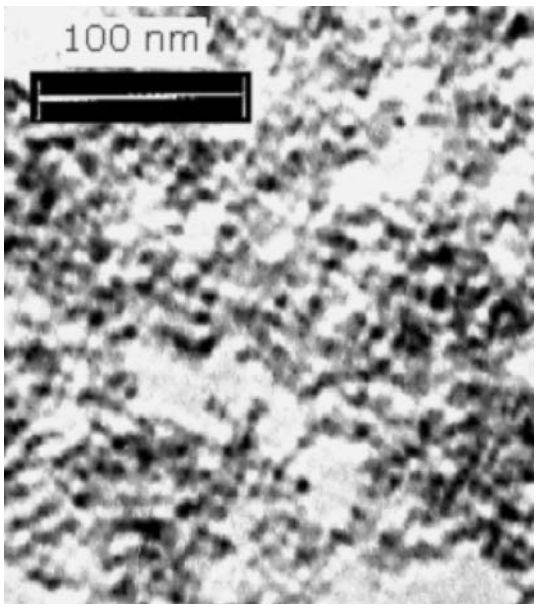

Fig. 3 TEM photograph of F-TiO2

Effect of pH values on the crystallization of F-TiO_2

Figure 6 shows the XRD patterns of F-TiO_2 sol particles prepared by sol-gel-crystallization process at 140 °C for 10 h in different applied pH situations. As shown in Fig. 6, the analyzed particles consisted of the anatase phase because the characteristic diffraction peaks of anatase (major peaks: 25.10°, 37.70°, 48.80°) were evident in the XRD spectrum of each sample. The change of the pH value

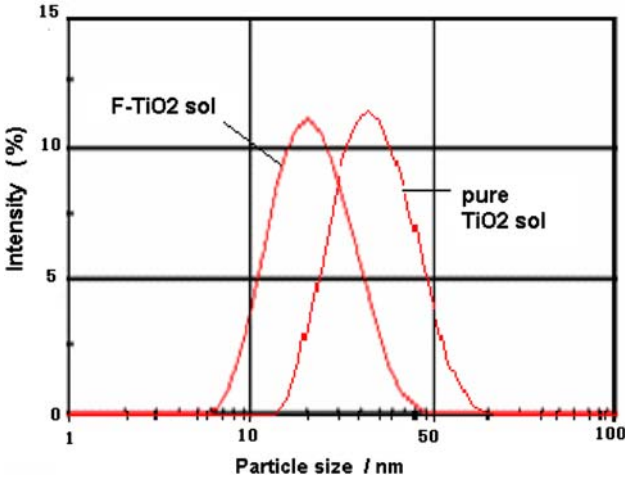

Fig. 4 PSD of TiO_2 sol sample

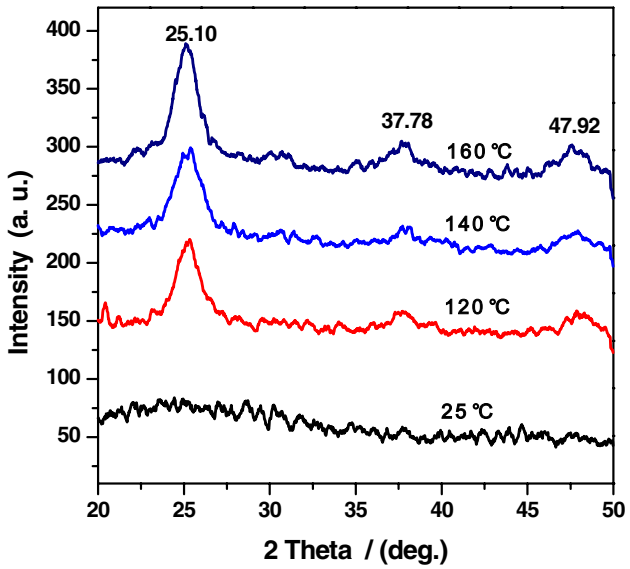

Fig. 5 Effect of temperature on the crystallization of F-TiO_2 sol particles

ranging from 0.8 to 3.5 during synthesis had little effect on the morphology of F-TiO_2. When pH $\leq$ 1.5, there was a small peak at $2\theta = 30.40°$ corresponding to the brookite phase of titania; When pH $\geq$ 4.0, the peptization of amorphous TiO_2 gel was not completed. After hydrothermal reaction, the obtained F-TiO_2 sol was instable.

Effects of F/Ti ratio in reactant on the crystallinity of TiO_2 sol particle

The relationship between the ratio of F/Ti in reactant and the crystallinity of TiO_2 sol particle prepared on the same hydrothermal crystallization conditions (140 °C for 10 h, pH value 1.2) was shown in Fig. 7. When the ratio of F/Ti

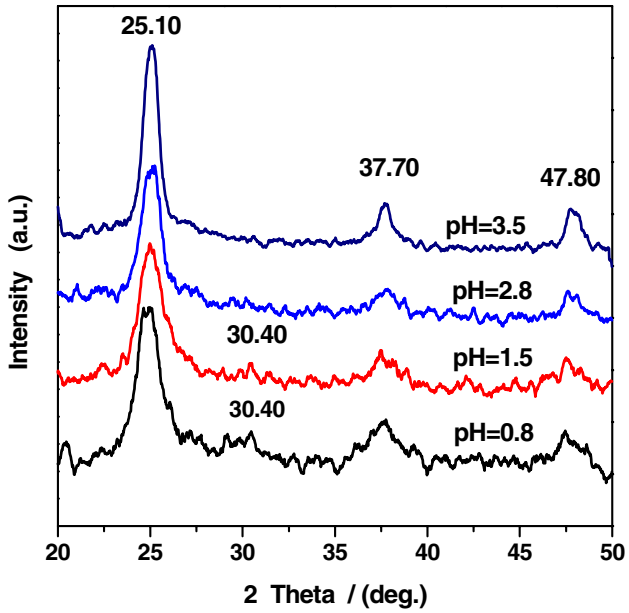

Fig. 6 Effect of pH values on the crystallization of F-TiO_2 sol particles

(at.) was in the range of 0.0–0.08, it was found that, the more the ratio of F/Ti, the higher the crystallinity of TiO_2 particles. The results showed that, under hydrothermal conditions, the addition of a small amount of anion F could help transform amorphous TiO_2 to anatase TiO_2 and enhance the crystallinity of TiO_2 significantly.

UV-Vis absorption of F-TiO_2

The absorption spectra of pure TiO_2, pure F-TiO_2 and sample F-TiO_2 sol prepared by the sol-gel-hydrothermal method and dried in a rotatory evaporator and dried in vacuum at 60 °C was shown in Fig. 8. It was found that sample F-TiO_2 could cause a new absorption band in the visible range of 400–600 nm apart from the fundamental absorption edge of TiO_2, which was located in the UV region at about 385 nm (shown in Fig. 8C); whereas, pure F-TiO_2 did not lead to any significant shift in optical absorption of TiO_2 (shown in Fig. 8B). This indicates that the doped F atoms in TiO_2 particles could not affect the optical absorption property of TiO_2 which was consistent with the result of F-doped TiO_2 reported by Li et al., who reported that the F-doping did not result in any significant shift in the fundamental absorption of TiO_2 [14]. Ammonium fluoride was used as a fluorine source in the process of sol-gel-hydrothermal crystallization, some nitrogen atoms of ammonium maybe entered the TiO_2 crystal lattice. Doping nitrogen led to narrow the band gap by mixing the N_{2p} and O_{2p} states and consequently inducing visible-light absorption [16]. Doping nitrogen induced the formation

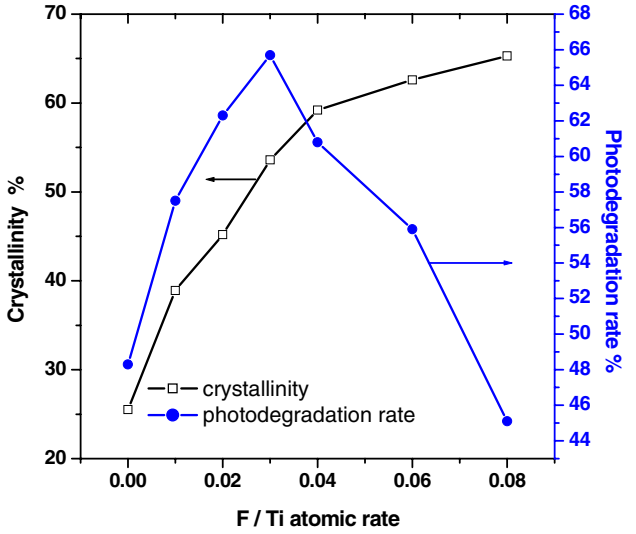

Fig. 7 Effects of F/Ti ratios on the crystallinity of F-TiO_2 sol and photodegradation rate of formaldehyde

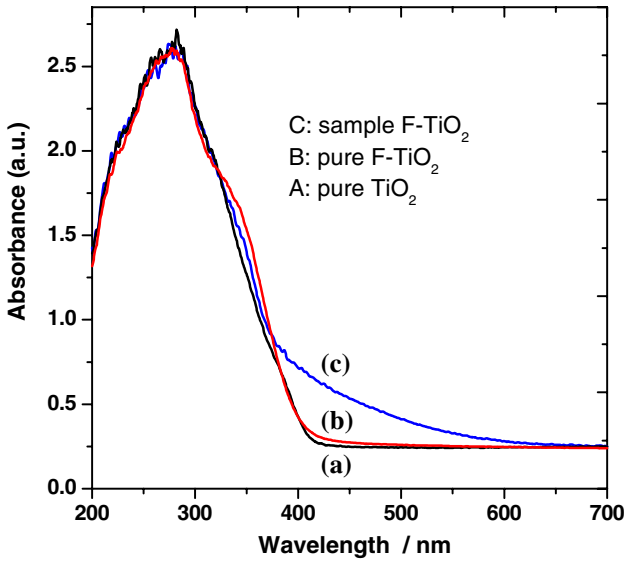

Fig. 8 UV–Vis–DRS spectra of TiO_2 sol dried in a rotatory evaporator and vacuum dried at 60 °C: A. pure TiO_2; B. pure F-TiO_2; C. sample F-TiO_2

of oxygen vacancies because two nitrogen atoms should replace three oxygen atoms for maintaining electroneutrality, and thus an oxygen vacancy formed in the TiO_2 crystal lattice. Oxygen deficient sites formed in TiO_2 particles were important for the Vis response to emerging [17]. Irie et al. reported that the isolated N_{2p} narrow band above the O_{2p} valence band was responsible for the visible light response to nitrogen doped TiO_2, when nitrogen was lightly doped (up to about 1%) into oxygen [18]. We had reported previously the visible light response to nitrogen and fluorine codoped TiO_2 powder prepared by solvothermal method was due to the isolated levels that consisted of N_{2p} orbital in the band gap of TiO_2 [5].

FT-IR Spectroscopy

FT-IR spectra of the TiO_2 sol particles were shown in Fig. 9. The TiO_2 sol particles showed the main bands at 400–700 cm^{-1}, which were attributed to Ti-O stretching and Ti-O-Ti bridging stretching modes. The small peak at 889.0 cm^{-1} was attributed to Ti-F vibration [13]. The peak at 1384.0 cm^{-1} was produced by NO_3^{-1}. The stronger peak at 1626.0 cm^{-1} was attributed to bending vibrations of O-H and N-H. The IR spectra of the sol sample dried at 110 °C revealed that Ti-O, Ti-F, N-H, Ti-OH, H-O-H groups existed in the as-prepared sample by sol-gel-hydrothermal method. The forming of Ti-F indicated that F atoms were incorporated into the TiO_2 crystal lattice.

XPS analysis

Figure 10 shows the XPS survey spectrum of the F-TiO_2 sol sample powder was prepared by sol-gel-hydrothermal processes. XPS peaks indicated that the F-TiO_2 sol sample powder contained Ti, O, F, N elements and a trace amount of carbon. The presence of carbon was ascribed to the residual carbon from the precursor solution and the adventitious hydrocarbon from the XPS instrument itself. At the same time, XPS data also showed that F and N elements were incorporated into the TiO_2 crystal lattice or adsorbed on the surface of the crystals. The total N and total F concentrations calculated from the XPS spectra were 0.8(at.)% and 2.0(at.)%, respectively.

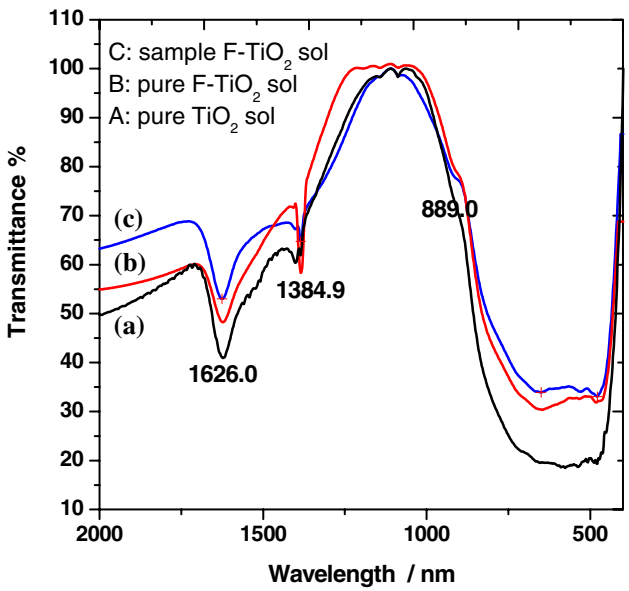

Fig. 9 FT-IR spectra of TiO_2 sol particles

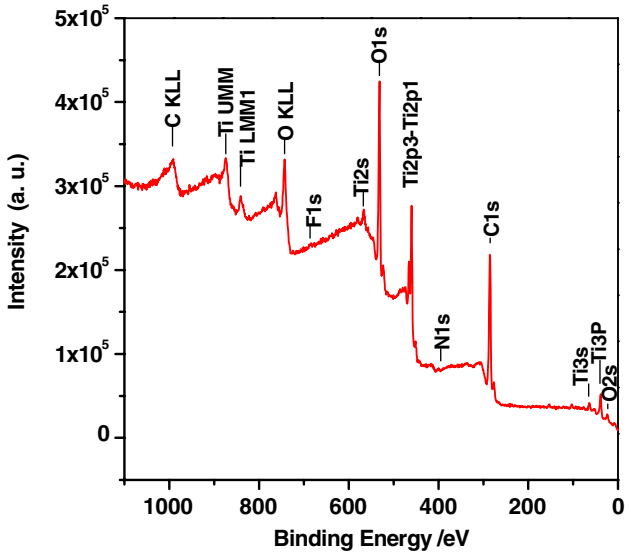

Fig. 10 XPS survey spectrum of F-TiO_2 sol sample dried and then calcined at 320 °C for 6 h

Figure 11 presents the F_{1s} XPS spectra of the F-TiO_2 sol sample powder after calcination at 320 °C for 6 h. The F_{1s} region was composed of two contributions. One symmetrical peak located at 685.5 eV originated from the F-containing compounds adsorbed on the surface of TiO_2 sol particles, however, the small peak located at 688.0 eV was attributed to the F atoms doped in TiO_2, i.e., the substitute F atoms that occupied oxygen sites in the TiO_2 crystal lattice. It was reasonable to assume that the small peak resulted from Ti-F bonds [13]. It showed that F atoms were incorporated into the TiO_2 crystal lattice by the sol-gel-hydrothermal method.

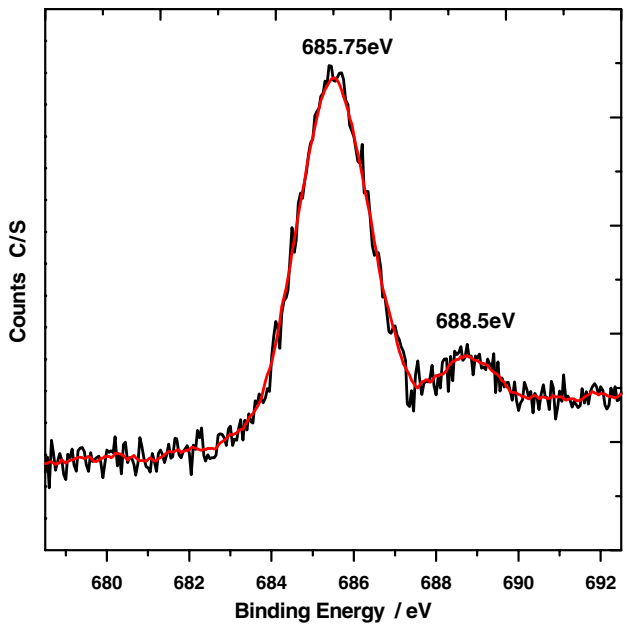

Fig. 11 F1s XPS spectra of F-TiO_2 sol sample dried and then calcined at 320 °C for 6 h

The adsorption capacity and number of acid sites

We determined the amount of surface acid sites of P25-TiO_2 powder, pure TiO_2 and F-TiO_2 sol particles by the titration method [15]. It was found that the amount of surface acid sites increased greatly after TiO_2 was doped with F atom. The increase of the acid sites on the surface of F-TiO_2 may be related to the higher electronegativity of fluorine, which tended to make the neighboring titanium atom more ''positively charged'', acting as lewis acidic sites, and interact with polarity organic compounds.

The amounts of formaldehyde, Rhodamine-B, and P-chlorophenol adsorbed upon P25-TiO_2 powder, TiO_2, F-TiO_2 sol particles were measured and shown in Table 1. It was found that the order of adsorption capacity for formaldehyde, Rhodamine-B, and P-chlorophenol was: P25-TiO_2< pureTiO_2 < F-TiO_2. The adsorption amount (A_{ad}) values were directly proportional to the surface acidities of samples: the stronger the surface acidity of TiO_2 particles, the more organic compounds was adsorbed. This result suggests that doping with F atom is an effective method to improve the adsorption capacity of TiO_2 for organic compounds.

Photocatalytic activity of F-TiO_2 sol

Activity of F-TiO_2 sol on photodegradation of formaldehyde

The photocatalytic activity of the F-TiO_2 sol was evaluated by photodegradation of formaldehyde. The F-TiO_2 showed good activity for the degradation of formaldehyde. Figure 12 presents the results obtained at 28 °C, flow rate 61 mL min^{-1} with relative humidity 54%. The degradation rate could be up to 74.5% at formaldehyde concentrations of 0.4 mg m^{-3}; under the same circumstance, the photodegradation rate of formaldehyde degraded by pure TiO_2 sol only to 62.1%. The addition of anion F could enhance the activity of catalyst significantly. At the same time, it was found that both degradation percentages of formaldehyde by pure TiO_2 sol and F-TiO_2 sol were decreased when the inlet concentration of formaldehyde was increased. The results indicated that the F-TiO_2 sol photocatalyst would be deactivated at higher concentration. Fig. 13

Effects of F/Ti ratio in TiO_2 on the formaldehyde degradation

A series of F-doped TiO_2 (the ratio of F/Ti (at.)) = 0.01, 0.02, 0.03, 0.04, 0.06, 0.08) sol was prepared sol-gel-hydrothermal method and on the same crystallization

Table 1 The adsorption capability and the amount of surface acid sites of TiO_2 (P25, TiO_2 and F-TiO_2)

Catalysts	Amount of HCOH adsorbed on TiO_2 (mmol/g-TiO_2)	Amount of P-chlorophenol adsorbed on TiO_2 (mol/g-TiO_2)	Amount of RHB adsorbed on TiO_2 (mol/g-TiO_2)	Amount of surface acid sites (mol/g-TiO_2)
P25	4.5×10^{-4}	4.35×10^{-4}	2.73×10^{-7}	0.076
TiO_2	1.26×10^{-3}	5.50×10^{-4}	3.68×10^{-7}	0.055
F-TiO_2	1.68×10^{-3}	7.42×10^{-4}	5.48×10^{-7}	0.128

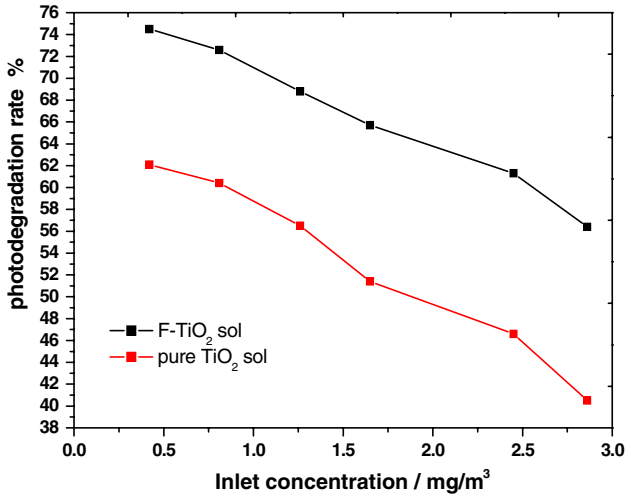

Fig. 12 Comparison of formaldehyde photodegradation rate by F-TiO_2 sol with that by pure TiO_2 sol

conditions (140 °C for 10 h, pH value 1.2). Photocatalytic degradation of formaldehyde measurement was at 28 °C, flow rate 61 mL min^{-1} with relative humidity 54%, the inlet concentration 1.65 mg m^{-3} and illumination source of a 11W FVL lamp. The relationship between the photodegradation percentage of formaldehyde and F/Ti ratio in TiO_2 was shown in Fig. 7. With the increasing F content in TiO_2, the photocatalytic activity of F-TiO_2 sol particles increased and reached the maximum at F:Ti = 0.03(at.). The increase in photocatalytic activity was ascribed to the promoting effect of fluorine ions on the crystallization of anatase TiO_2 during hydrothermal crystallization and then improved the crystallinity of TiO_2 sol particles.

It could be seen from Fig. 7 that the 0.03F-TiO_2 sol was the highest photocatalytic activity which was 1.4 times of pure TiO_2 sol. It was reported that an appropriate amount of F ions doping might slow the radiative recombination process of photogonerated electrons and holes in TiO_2 [14] and lead to the formation of new active site [19]. The results of Table 1 indicate that TiO_2 doped F atoms would cause the increase in acid sites on TiO_2 surface, which might thus promote its adsorption capability for formaldehyde because of the enhanced interaction between the surface acid sites and formaldehyde molecules and further enhance the photocatalytic activity.

With the increase of further fluoride concentration, when F: Ti (at.) was higher than 0.03, the degradation percentage of formaldehyde started to decrease. Although the increase of fluorine concentration in TiO_2 could give rise to the improvement in the crystallinity of TiO_2 sol particles, when the fluorine was too high, the diminution of the surface hydroxyl of TiO_2 (≡Ti-OH) would decrease the ability to trap the holes [19]. In addition, the depletion of ≡Ti-OH would inhibit the formation of surficial peroxide and fluoride anion was well-known as the inhibitor of complex formation between $Ti^{4+}$and peroxide. The displacement of –OH by F changed the adsorption and the surface interactions, especially for formaldehyde molecules that interacted with –OH groups, the active sites were held by F^- anions [20]. On the other hand, fluorides strongly adsorbed to the TiO_2 surface and interfered with adsorption

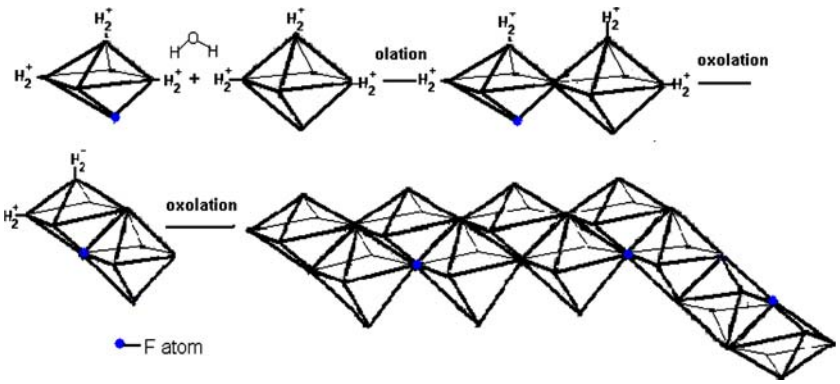

Fig. 13 Proposed mechanism for the formation of anatase TiO_2. Fluorine atoms combined with Titanium to form asymmetric TiO_6 octahedra; two octahedral join at a vertex forming a dimmer and then link along a polar edge; dimmer coalescent along polar edge to form a zigzag chains of octahedral (basic structural unit of anatase)

of formaldehyde. The photocatalytic activity of TiO_2 decreased after surface fluorination with fluoromethane [21].

Mechanism of anatase F-TiO_2 crystallization

The titanium in the initial tetra butyl titanate has 4-fold co-ordination, when the tetra butyl titanate reacts with water, the titanium ion increases its co-ordination by using its vacant d-orbital to accept oxygen lone pairs from nucleophilic ligands (such as OH groups) by co-ordination expansion. Consequently, titanium ions in solution exist as 6-fold co-ordinate structures. In the present study, the reaction was performed in an acidic medium, the groups of –OH, NH^{4+}, and F^- would be presented and the composition of this solution was $[Ti(OH)_xF_y(OH_2)_{6-x-y}]^{(6-x-y)+}$. These 6-fold structural units underwent condensation and became the octahedral that was incorporated into the final amorphous gel structure.

In the present research, HNO_3 should disperse the aggregated TiO_6 octahedra and the related species in the amorphous phase into discrete TiO_6 octahedra by proton adsorption on the surface of these amorphous precipitates making them positively charged. The result of electrostatic repulsion causes larger particles to break into smaller particles until an equilibrium size reaches. At the same time, according to the date of XPS experimental, fluoride ions strongly interact with amorphous TiO_2, tend to displace the surface –OH groups and coordinate directly the titanium atoms [22], which would cause the transfiguration of TiO_6 octahedra and decrease of the surface charge of Ti^{4+}. In the process of hydrothermal crystallization, two discrete single TiO_6 octahedral join at corner through oxolation initially (as shown in Fig. 9) [23]; by further condensation, they would become joined along an edge to form a dimer, as the cation–cation repulsion causes the centers of the two octahedral to move apart, the shared edge becomes shorter [24]. Owing to the doping of fluoride, few TiO_6 octahedral deformed and formed polarity surface and edge. The dimers tend to form screw chains of polymer by sharing polarity edge with further oxolation reaction, which were similar to anatase in structure, and the screw chains can form the anatase nuclei by oxolation reaction. Another possibility is that two opposite edges of each dimer are shared forming a linear chain along the (001) direction (basic structure unit of rutile) [25]. But in the present study, it is difficult to bond two dimers with two opposite edges, because the doping of fluorine in TiO_6 octahedral leads to the structure of TiO_6 octahedral deformation and dissymmetry. The third possibility is that dimers are bonding through corner-shared and polar edges to form the structure of brookite that is slightly complicated [26].

Conclusion

An anatase fluoride doped TiO_2 sol (F-TiO_2) catalyst was fabricated by a sol-gel hydrothermal method using tetra butyl titanate as a precursor. After doping with fluorine, the crystallinity of TiO_2 sol particles was increased, the adsorption capacity and photocatalytic activity was enhanced. The as-prepared TiO_2 sol could form uniform thin films onto various kinds of substrate materials by spraying, dipping or brushing drying at room temperature.

On the same hydrothermal reaction conditions, when F:Ti = 0.03(at.), the photocatalytic activity of F-TiO_2 sol particles reaches the maximum, which was 1.4–1.8 times of pure TiO_2 sol prepared in the same conditions.

Formed mechanism of anatase F-TiO_2 under hydrothermal conditions was possibly as follows: owing to the doping of fluoride, few TiO_6 octahedral deformed and formed polarity surface and edge; two discrete single TiO_6 octahedral join at corner through oxolation initially, by further condensation, they would become joined along polarity edges to form a dimer, the dimers tended to form screw chains of polymer by sharing polarity edge with further oxolation reaction, which were similar to anatase in structure and the screw chains could form the anatase nuclei by oxolation reaction.

Acknowledgement We gratefully acknowledge the financial support of Guangdong Natural Science Foundation (020863 and 036555).

References

1. Lee DS, Liu TK (2002) J Sol-Gel Sci Tech 25:121
2. Assmann SE, Widoniak J, Maret G (2004) Chem Mater 16:6
3. Fu GF, Vary Patricia S, Chhiu-Tsu Lin, J Phys Chem B, 109 (2005) 8889
4. Scalfani A, Palmisano L, Schiavello M (1990) J Phys Chem 94:829
5. Huang DG, Liao SJ, Liu JM, Dang Z, Petrik Leslie (2006) J Photochem Photobio A: Chem 184:282
6. Ekabi AH, Serpone N (1988) J Phys Chem 92:5726
7. Lee JH, Kang M, Chong SJ (2004) Water Res 38:713
8. Choi HJ, Choi US, Han YS, Hong YG, Huh GU, Kwon CH, Lee SH, Na HS, Choi WS, US6576589, 2000.09.19
9. Gao L, Zhang YQ, Sun J, CN1295977, 2001.5.23
10. Choi YS, Jun MS, Un MS, Noh CS, O B Yang, KR2003043536, 2003.1.2
11. Xie YB, CW Yuan, Li XZ (2005) Mater Sci Eng B 117:325
12. Kim HY, Park GS, Yang JS, KR 2003021291-A, 2003.3.15
13. Yu JC, Yu JG, Ho WK, Jiang ZT, Zhang LZ (2002) Chem Mater 14:3808
14. Li D, Haneda H, Hishita S, Ohashi N, labhsetwar NK (2005) J Fluorine Chem 126:69
15. Benesi HA (1957) J Phys Chem 57:970
16. Asahi R, Morikawa T, Ohwaki T, Aoki K, Taga Y (2001) Science 293:269
17. Ihara T, Miyoshi M, Iriyama Y, Matsumoto O, Sugihara S (2003) Appl Catal B: Environ 42:403

18. Miyauchi M, Ikezawa A, Tobimatus H, Irie H, Hashimoto K (2004) Phys Chem Chem Phys 6:865
19. Minero C, Mariella G, Maurino V, Pelizzetti E (2000) Langmuir 16:2632
20. Allèn JA, Peiró AM, Saadoun L, Vigil E, Domènech X, Peral J (2000) J Mater Chem 10:1911
21. Sun RD, Nishikawa T, Nakajima A, Nakajima A, Watanabc T, Hashimoto K (2002) Polym Degr Stabil 78:479
22. Yin HB, Wada YJ, Kitamura T (2001) Mater Chem 11:1694
23. Assmanna SE, Widoniak J, Maret G (2004) Chem Mater 16:6
24. Gopal M, Moberlychan WJ, De Jondhe LC (1997) J Mater Sci 32:6001. DOI: 10.1023/A:1018671212890
25. Yanagisawa K, Ovenstone J (1999) J Phys Chem B 103:7781
26. Cheng HM, Ma JM, Zhao Z, Qi LM (1995) Chem Mater 7:663